IOP Publishing Flexible and Printed Electronics
Journal *Flex.Print.Electron.* (XXXX) XXXXXX https://doi.org/XXXX/XXXX

Thermoplastic elastomer composite filaments for strain sensing applications extruded with an FDM 3D printer

Antonia Georgopoulou[1,2], Tutu Sebastian[1], Frank Clemens[1]

[1]Department of Functional Materials, Empa – Swiss Federal Laboratories for Materials Science and Technology, Überlandstrasse 129, 8600 Dübendorf, Switzerland
[2]Department of Mechanical Engineering (MECH), Vrije Universiteit Brussel (VUB), and Flanders Make Pleinlaan 2, B-1050 Brussels, Belgium.

E-mail: antonia.georgopoulou@empa.ch , frank.clemens@empa.ch

Received xxxxxx
Accepted for publication xxxxxx
Published xxxxxx

Abstract

The use of thermoplastic elastomers with conductive fillers enables to produce strain sensors in a variety of shapes and forms by using thermoplastic processing routes. However, some methods of thermoplastic processing are costly and require long production time. Filament printing, an additive manufacturing route that still exhibits a high annual growth rate, is a cost and time-efficient method of additive processing. In this study a commercial conductive thermoplastic polyurethane (TPU) based fused deposition modelling (FDM) filament and a styrenic block co-polymer (TPS) compound were extruded through two different FDM based nozzles sizes, using an FDM 3D printer. The TPU material could only be extruded through a 0.5 mm orifice, using a lower nozzle diameter resulted in a none-elastic brittle filament. For the TPS material it was possible to produce filaments with diameter 0.3 mm and 0.5 mm. In all dynamic tests, the extruded commercial piezoresistive TPU filament either showed at higher elongation plastic deformation, which resulted in resistance uncertainty at low strain, or a secondary peak in the resistivity measurement. For the TPS material, mainly the relaxation of the material resulted in lagging of the resistive value at low strain, because of the buckling of the fiber. Using combined dynamic and static measurements, a reproducible signal could be achieved with the TPS based material, while the TPU based material could not be used as a sensor in this area of strains.

Keywords: thermoplastic elastomer-based fiber, soft strain sensor, piezoresistive behavior, FDM 3D printer

1. Introduction

The rapid advancement in the field of soft robotics and wearable electronic devices calls for the development of soft, stretchable sensors that are able to conform to complex structures and geometries [1–8]. Typically, soft sensor materials are extrinsic conductive composites, consisting of an elastomeric material and a conductive filler like graphite, carbon black, carbon nanotubes, nanofibers or graphene [9–12]. In the case of soft material strain sensors, the stretchability is a crucial characteristic of the sensor performance. In comparison to thermoplastics, resin or metal-

based gauge sensors, soft elastomer-based sensors are able to endure large elongations.

In comparison to pure elastomers, thermoplastic elastomer-based piezoresistive sensors become more and more popular, because they can be easily shaped by different processing routes like warm pressing, extrusion, injection molding and filament printing, an additive manufacturing route which still exhibits high annual growth rate [13]. Block copolymer elastomers like styrene-ethylene-butadiene-styrene tri-block copolymer (TPS), are a common material option for the fabrication of conductive composites and stretchable electronic devices [14]. Thermoplastic polyurethane (TPU) is another common option as a matrix material in conductive composites for sensing applications [8, 9].

Sensors containing thermoplastic elastomers like TPU and TPS are found in many forms such as filaments [16–19]. Filaments can be implemented in textiles and complex conforming structures and are particularly important in cases like continuous vital function monitoring. A diameter of 0.3 mm for the sensor filament, to monitor vital functions and body movements, was optimal for manual fabrication process and it has sufficient sensitivity to measure pulse signal at the wrist and large body movements during sport activities [20, 21]. Piezoresistive sensor filaments based on conductive composite elastomers with high carbon black concentration have been reported to have a very good dynamic response and low signal relaxation [22]. The concentration of the carbon filler affects the conductivity and the signal response of the soft matter sensor composite material [23].

It has been reported that filaments made from TPU and a carbon filler had good sensitivity for a range of strains of over 320% [24]. However, a loss of linearity in the form of a secondary peak was observed at the unloading, during dynamic tensile testing. The appearance of a secondary peak isn't uncommon in conductive composites based on TPU [11,12]. A similar secondary peak at the unloading was observed by Zhang et al. for their TPU /MWCNTs sensor, especially at higher strains [27]. It has been suggested that this secondary peak originated from the destruction and reconstruction of the conductive networks during the loading and unloading [13]. Ji et al. have also explored soft matter sensor filaments based on TPU/carbon black and TPS/carbon black. They observed, that even though the TPU based system had better dispersion of the filler, the TPS system had better sensitivity [28]. Drozdov et al. observed, that samples strained with higher strain rates, had increased conductivity compare to samples strained at a lower strain rate [29].

Stretchable electronics like wearable devices require complex geometries and at the same time optimal sensor performance [30]. Conductive elastomers have already developed for the 3D printing process to fabricate complex sensor structures with good sensor properties like sensitivity, reliability, good linearity, low hysteresis and the ability to reach high elongations [25]. Conductive filaments for fused deposition modeling (FDM) process are used to build up complex electronics structures and attract interest for several applications [26]. TPU based conductive filaments show good conductivity and very high sensitivity (GF up to 400) [27]. Typically fused filament fabrication (FFF) /fused deposition modeling (FDM) 3D printing is based on the extrusion of filaments with a diameter of 1.75 and 2.85 mm [31].

In this attempt, piezoresistive thermoplastic elastomers were extruded into filaments with the method of extrusion using a commercial 3D printer. The method of using a commercial FDM 3D printer for the extrusion of fibers has been seen before in the case of optical fibers with encouraging results [32]. In this attempt, the same method of extruding fibers through an FDM 3D printer nozzle was applied for the case of piezoresistive, elastomer strain sensor filaments. A commercial TPU based flexible conductive and an earlier developed TPS based conductive feedstock was used in this study. The use of commercial materials has the important advantage that the material is readily available in the market. In order to evaluate the pure piezoresistive properties, the filaments (FDM of a monofilament) were fixed in a tensile testing machine and the sensor behavior was investigated until breakage, under dynamic and combined dynamic and quasi-static conditions.

2. Experimental

2.1 Empa Filaments: Compounding and Extrusion

A styrene-ethylene/butylene-styrene triblock copolymer was obtained by Kraiburg TPE (Waldkraiburg, Germany) and carbon black ENASCO 250 was obtained from TIMCAL (Bodio, Switzerland). The materials were mixed in a mass ratio of 1:1 using a torque rheometer from Thermofisher (Durlach, Germany). The optimizing of the concentration for the TPS/carbon black composite was explored in a previous study [21]. Using the capillary rheometer Rosand RH7(Malvern Instruments Limited, Malvern, United Kingdom) filaments with 1.75mm were extruded. For the extrusion of the sensors, a Pro 2 Dual Extruder 3D printer (Raise 3D, Irvine, United States of America) was used. FDM dies with a diameter of 0.3 mm and 0.5 mm were used to fabricate the monofilament at 180°C. Filaments with diameters 0.3 mm and 0.5 mm were produced using the same conditions.

2.2 Eel Filaments: Extrusion

The commercial TPU conductive filament Ninjatek Eel was supplied by Ninjatek Fenner Drives (Manheim, USA). This filament is available with a diameter of 2.85 and 1,75 mm and has a carbon black filler content of around 18% w/w [33]. Using a hot-end with nozzles with diameter below 0.5 mm, resulted in brittle filaments which broke at 15% strain and

could be therefore not been used as elastic strain sensors. The temperature of the nozzle during the extrusion was 220 ºC.

2.3 Optical analysis

The diameter of the filaments was confirmed with multifocal optical microscopy, using a Zeiss Stereo Discovery microscope (Carl Zeiss Microscopy, Jena, Germany).

2.4 Tensile Testing

The mechanical and electrical behavior of the sensor during straining was performed with tensile testing. The sensor response was assessed during tensile test up to the breakpoint as well as for cyclical and quasi-static testing. The tensile testing was performed using a Zwick Roell Z005 tensile testing machine (ZwickRoell, Ulm, Germany) with a 200 N load cell. Pneumatic clamps with a pressure of 4 bars were used. In order to assess the piezoresistive response of the filaments, simultaneously the strain and the electrical resistance were measured. For a piezoresistive analysis, a Keithley 2450 (Keithley Instruments, Solon, USA) multimeter was used.

A filament length of 130mm was used to be able to fix the filaments in between the pneumatic clamps with self-designed carton frames to avoid slipping at higher strains. The gauge length between the two pneumatic clamps was fixed to 50 mm and three different strain rates, 50, 100 and 200 mm/min were used for the tensile test until breakage. For all cycling tests, a constant strain rate of 100 mm/ min was used. For the dynamic test, 10 cycles between 0 and 70% strain were performed. The quasi-static test involved five cycles of loading and releasing with a dwell time of 60s at strain 15% and 35%. For calculating the piezoresistive response of the filaments, the value relative resistance was used:

$$R_{rel} = \frac{R-R_0}{R_0} \quad (1)$$

Where R_{rel} is the relative electrical resistance, the electrical resistance (R) is the value measured during the testing and R_o is the value at the beginning of the tensile test (unstrained filament). The Gauge factor (GF) is defined as:

$$GF = \frac{R_{rel}}{\varepsilon} \quad (2)$$

Where ε is the value for the strain.

During cycling testing, the drift of the electrical sensor signal was calculated at a fixed strain between two different cycles. The hysteresis was calculated at a fixed strain during the loading and the releasing phase of the same cycle. The uncertainty is defined as the strain area, were the sensor loss sensitivity. In other words the same electrical signal can be achieved for different strain values. The relaxation was calculated as a difference of the mechanical or electrical signal at the begging and end of the dwell time during quasi-static testing.

3. Results and Discussion

3.1 Optical analysis of FDM printed monofilament

The diameter of the filaments was confirmed with multifocal optical microscopy) under magnification 20x (figures 1a and 1c).

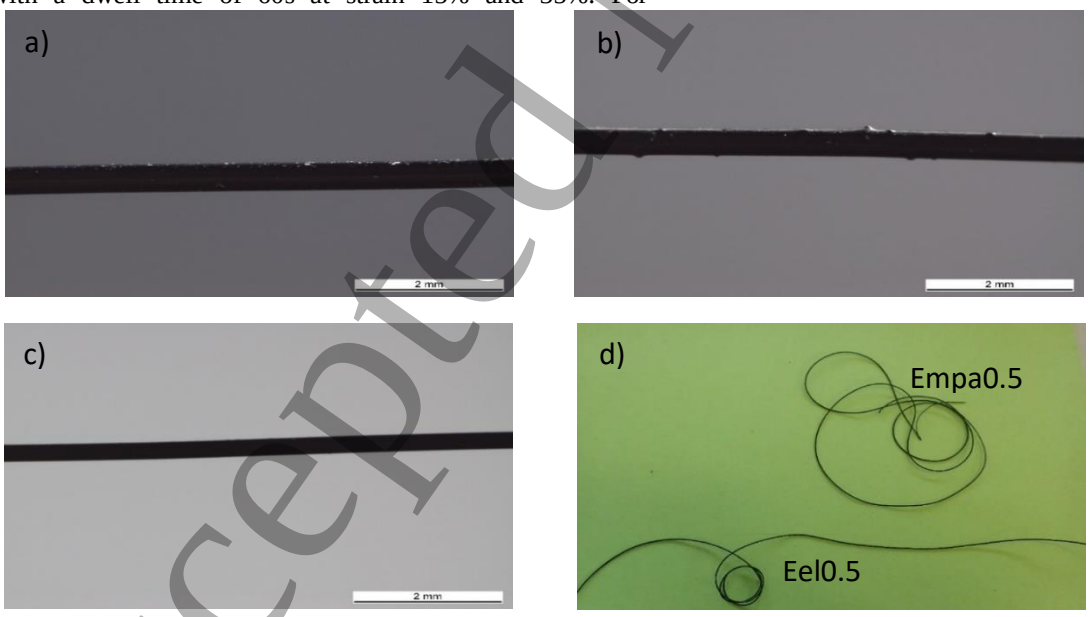

Figure 1: The piezoresistive elastomer monofilament strain sensors a) Empa0.5 b) Eel0.5 c) Empa0.3 under magnification x20. The diameter of the filaments was assessed with an optical microscope. d) Longer pieces of filament Empa0.5 and Eel0.5 filaments are presented.

In Figure 1 it can be seen, that surface of the Empa0.3 and Empa0.5 filaments is very smooth, whereas Eel0.5 has particles on the surface of the monofilaments.

3.2 Tensile test up to fracture: Mechanical Behavior

For the tensile testing until breakage, the monofilaments were tested with three different strain rates, 50, 100 and 200 mm/min. The Gauge factor was calculated for every linear part in the resulting strain-resistance curve. The most important characteristic values of mechanical behavior can be seen in table 1. For the three different strain rates, the stress, and strain at the yield point and the breakpoint were compared for the different filaments. In addition, the Young's modulus at low strain was investigated.

Table 1: Mechanical properties for the three conductive filaments at different strain rates.

Filament	Strain Rate (mm/min)	Stress at yield point (MPa)	Strain at yield point (%)	Stress at breakpoint (MPa)	Strain at breakpoint (%)	Young's modulus (MPa)
Empa0.3	50	4.9	11	11.0	206	34
Empa0.5	50	5.2	13	4.1	150	35
Eel0.5	50	4.6	12	18.9	493	33
Empa0.3	100	5.1	12	9.0	166	35
Empa0.5	100	4.2	10	9.5	161	35
Eel0.5	100	4.6	13	20.4	494	34
Empa0.3	200	5.3	13	10.4	183	86
Empa0.5	200	5.5	13	5.3	150	98
Eel0.5	200	9.4	15	27.5	360	144

At the lower strain rates of 50 mm/ min and 100 mm/ min, similar mechanical behavior for all the three filaments could be observed. Especially, when looking at the stress and strain at the yield point, all the three filaments showed stress between 4 and 5 MPa and strain between 12% and 13%. In the case of the Empa fibers, as it can be seen in Figure 2, the yield point can be distinguished more prominently (like thermoplastic (semi-crystalline materials), whereas the Eel filament show typical elastomer behavior (Figure 2).

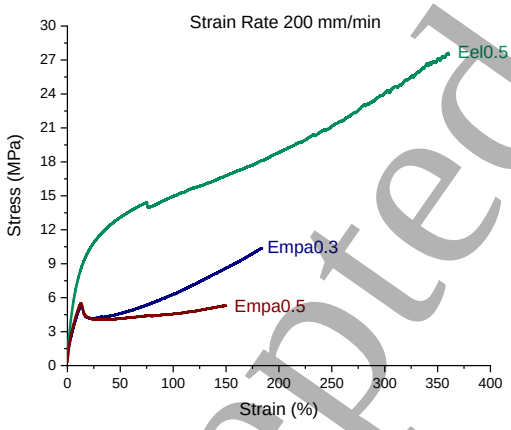

Figure 2: Stress-Strain Response to the breakpoint for the filaments Empa0.3, Empa0.5, and Eel0.5.

The Young's modulus at the lower strain rates of 50 mm/ min and 100 mm/ min was similar for the three sensor filaments. The Young's modulus at the 200 mm/min strain rate increased significantly (see Table 1). For the Empa filaments, at the highest strain rate, the elasticity modulus was three times higher, whereas for the Eel0.5 mm filaments, it was more than 4 times higher. This dependence of the Young's modulus on the strain rate has been reported in the case of elastomers and their composites [34]. Kanyanta and Ivankovic, observed for thermoplastic polyurethane an increase of the Young's modulus at higher strain rates, while at low strain rates the dependency was not significant [27].

Looking at the stress and strain at the breakpoint, the Eel0.5 filament could endure very large elongations of up to 400%, which is almost double of the Empa filaments could endure. This fact can be explained by the lower carbon black content of the Eel0.5 filament. The Eel0.5 filament contains 18% w/w carbon black, while the Empa filaments contain 50% w/w carbon black. The higher carbon black percentage can justify the brittleness of the Empa filaments compare to the Eel filaments.

3.3 Tensile test until fracture: Electrical Behavior

Looking at the piezoresistive response of the three sensor filaments, the gauge factor was calculated to describe the sensitivity of the different filaments (Table 2).

Table 2: The gauge factors calculated at the linear parts of the sensor response during a tensile test for the different filaments and the different strain rates.

Filament	50 mm/min		100 mm/min		200 mm/min	
Empa0.3	GF=43 GF=12 GF=4	ε=0-50% ε=51-120% ε=121-206%	GF=29 GF=52	ε=0-122% ε=123-166%	GF=144 GF=158	ε=0-122% ε=122-183%
Empa0.5	GF=21 GF=4 GF=31	ε=0-80% ε=81-130% ε=131-149%	GF=1 GF=14	ε=0-74% ε=75-161%	GF=46 GF=115	ε=0-124% ε=124-161%
Eel0.5	GF=1 GF=0.003	ε=0-234% ε=235-422%	GF=5	ε=0-494%	GF=1 GF=3 GF=4 GF=7	ε=0-140% ε=141-210% ε=211-251% ε=252-361%

The gauge factor as a measure of the sensitivity was calculated on the linear parts of the plot relative resistance and strain as it can be seen in figure 3.

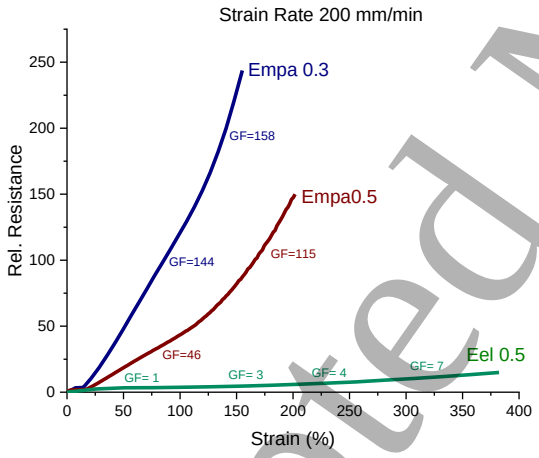

Figure 3: Piezoresistive sensor response of the three filament sensors and the calculation of the gauge factor at the linear parts of each curve.

Both Empa 0.3 and Empa0.5 have better sensitivity than the Eel0.5 in all the different strain rates, a fact that can be interpreted by the higher concentration of carbon filler in the Empa filaments. Increasing the strain rate, resulted in increased sensitivity, especially in the case of the strain rate of 200 mm/min. The fact that higher strain rates lead to higher sensitivity has also been reported by Qi and Boyce [35]. The Empa0.3 presented the highest sensitivity at all strain rates and in most of the strain rates. At strain rate 200 mm/min, the Empa0.3 filament exhibited an exceptional sensitivity, with a gauge factor of 158 for strains up to 150%, being able with this exceptional sensitivity to detect even small changes in strain. On the other hand, Eel0.5 had a very low gauge factor and based by many authors, this low sensitivity will be a disadvantage for the performance of the filament as a strain sensor.

3.4 Dynamic cyclic testing

Dynamic testing is typically used to investigate sensor response. The reproducibility of the electrical signal between each cycle, linearity and the hysteresis of the sensor signal can be investigated with this test method. The loss of linearity (uncertainty) can be exhibited in the form of a secondary peak. Therefore dynamic test is a useful assessment to investigate the appearance of such secondary peak.

Therefore, dynamic tensile tests involve cyclical loading and releasing. The test with 10 cycles was performed for all the filaments at the range of stain 0-70% (figure 5).

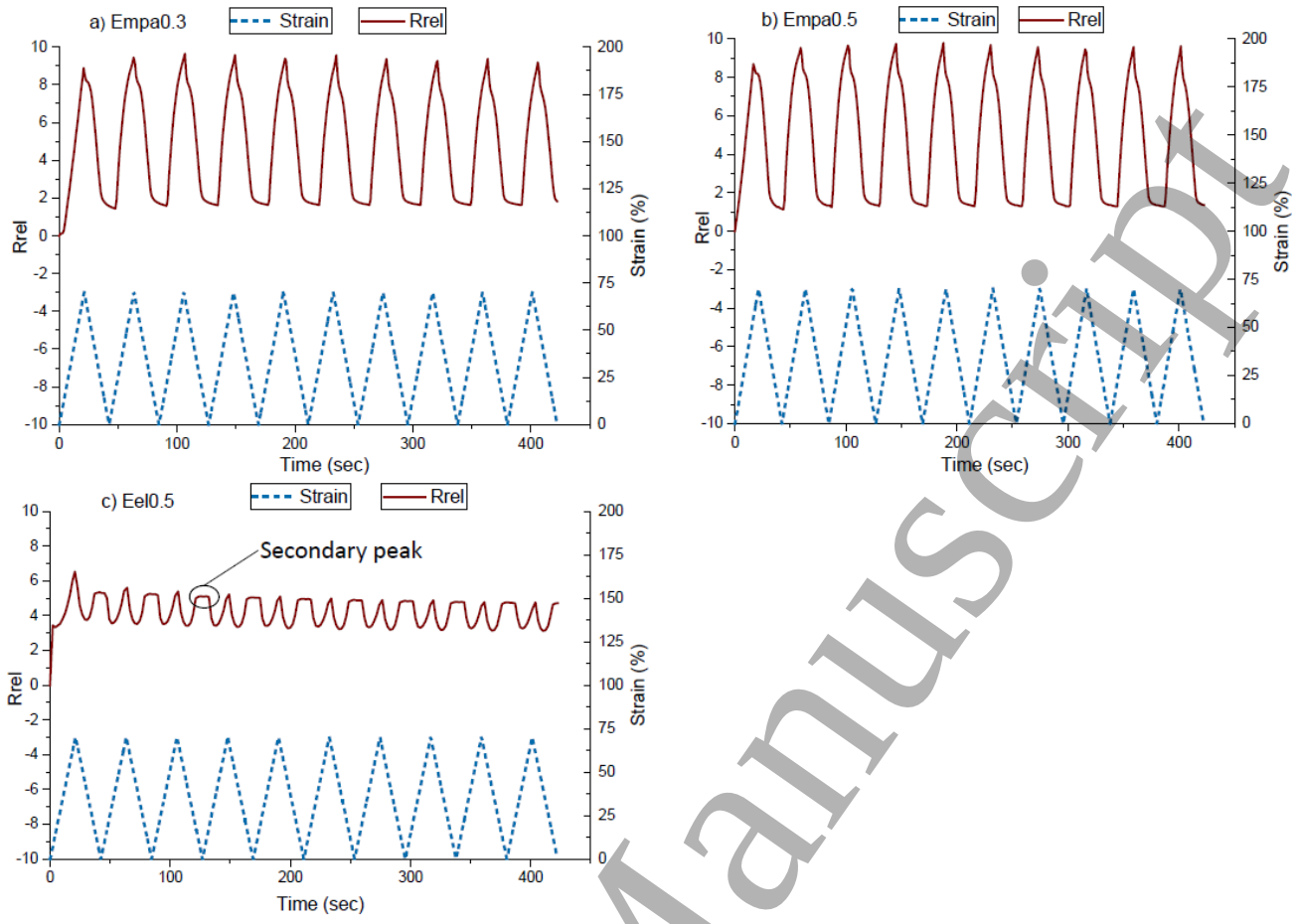

Figure 4: Dynamic cyclical tensile testing in the strains 0-70% for the monofilament sensor filaments a) Empa0.3 b) Empa0.5 c) Eel0.5.

From the dynamic test, important aspects can be extracted about the sensor behavior like the signal drift and the sensor response during straining and releasing. The signal drift is an important factor that shows the offset of the sensor signal from the expected trend between the different numbers of the dynamic cycles [39] and has significant importance for the long-term performance of the system. Because of the yield point of the two Empa filaments (see Fig. 2), the signal response was different for the first cycle. After the second cycle, the signal became stable between each cycle. Therefore, for the Empa filaments, the lager drift between the first and second cycle can be avoided by pre-straining the filament [22]. During loading and the releasing phase of the dynamic tensile test the sensor can lose linearity (e.g. hysteresis), this would imply uncertainty in the function of the electrical response for the specific range of strain. Table 3 shows the data for the drift and the uncertainty of the sensor function for the three filament sensors.

Table 3:Electrical Drift, hysteresis and the uncertainty of the Empa and Eel filaments. The drift was calculated between the second and last cycle and between two consequent cycles.

FDM extruded filament	Drift between 2 and 10 cycle		Drift between 9 and 10 cycle		Hysteresis at 4% strain	Secondary peak	Uncertainty
	@ 0% strain	@ 70% strain	@ 0% strain	@ 70% strain	@ 46% strain*		
Empa0.3	8%	4%	5%	2%	25%	-	< 14% strain
Empa0.5	1.5%	1%	1.5%	0.4%	47%	-	< 26% strain
Eel0.5	10%	16%	0.6%	0.2%	23%	At 45% strain	< 45% strain

* Because of the behavior of the Eel filaments during the dynamic test.

In the case of the Empa0.3 it can be seen (figure 5a) that the relative resistance followed the change the strain. Only at low strains, in the unloading, a plateau can be observed. This plateau appears at strains lower than 14% and 26% for the Empa0.3 and Empa0.5 monofilament, respectively. Visually a buckling was observed during the measurements. This could explain, that the plateau which could be observed during the dynamic measurements was caused by the plastic deformation which occurs by stretching the filaments above the yield point.

The drift of the sensor signal was lower in the case of the Empa0.5 filament at high and low strains, compared to the Empa0.3 filament (see Table 3). However, when looking at the hysteresis (calculated at 46% strain) of the electrical response, the Empa0.5 filament with 47 % hysteresis surpassed the Empa0.3 (25.4% hysteresis).

In the case of the Eel0.5 filament (figure 4c), the drift between two subsequent cycles (9^{th} and 10^{th}) was the lowest. The hysteresis for the Eel0.5 was also the lowest (see Table 3). However, the electrical response of the Eel0.5 filament during the unloading of the first cycle the electrical signal behavior change completely. The further increase in resistance during the first unloading phase results in a further increase of the electrical resistance. A possible explanation for this phenomenon is, that during the first cycle the conductive filler will be oriented and distance between the particles will increase as discussed by Flandin et al [36]. This will result in an increase in the electrical resistance (e.g. rel. resistance) as shown in Figure 5. Tang et al. described that the sensor behavior of conductive elastomer sensor materials can be affected by the viscoelastic behavior of the matrix [37]. Because of the viscous part, the entanglement of the elastomer chains, during the unloading, will result in a hindering of the reconstruction of the carbon filler network. For the Eel0.5 filament, at 46% strain, the resistance increases until a plateau occurs. The origin of this secondary peak has been already discussed in the literature. Duan et al. and Tang et al. explain this phenomenon by the construction and reconstruction of the conductive network [37] and the viscoelastic nature of the elastomer matrix [38]. The increase of resistance (secondary peak) during the unloading part of the dynamic test is repeatable in each cycle. Strain analysis with secondary peaks are not easy to validate. For example, as it can be seen in figure 4c, a value of relative resistance of 2.5 corresponded to a strain value of 50% during the loading phase of a cycle, but during the unloading phase, this value corresponded to the strain values of 61%, 21% or 2.4%.

3.5 Quasi-static cycle testing

Another important aspect of piezoresistive elastomer strain sensors is the mechanical and electrical relaxation and drift when static strain occurs during the application. Thermoplastic elastomers, like styrene-ethylene-butadiene triblock copolymer (TPS), thermoplastic polyurethane (TPU, and their composites are susceptible to stress relaxation phenomena [39]. In order to assess the relaxation and drift, the cyclical test was repeated, but in this case, a dwell time of 60 sec at the maximum and minimum strain value was included in the test procedure. The filaments were cycled 5 times between 15-35%. Figure 7 shows the results of these measurements for the Empa filaments.

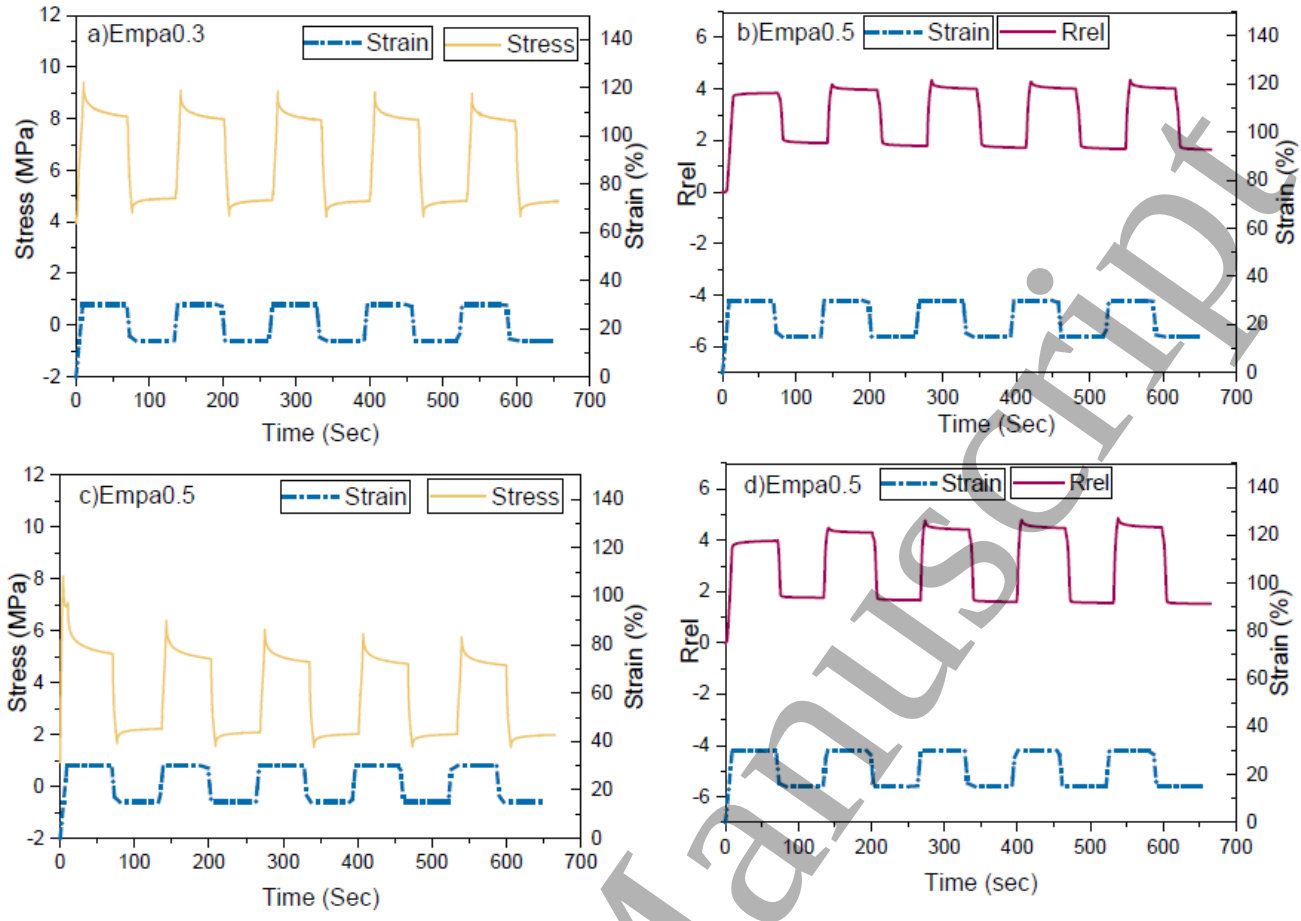

Figure 5: Quasi-static cycle testing, in a range of strains 15-35% with a holding phase of 60s between loading and releasing for the Empa monofilament filaments a) Stress Response for the Empa0.3 filament b) Relative resistance response for the Empa0.3.

Similar to the dynamic cycle testing, the relative resistance followed the change in the strain for the loading and the unloading phase in each cycle. For the empa0.3 filament, the response was stabilized after the third cycle. Because of the relaxation of the thermoplastic elastomer material, a change in the mechanical and the electrical signal can be observed during the dwell time. At high and low strain, the relaxation for the stress was quite similar (table 4).

Table 4: Mechanical and Electrical Relaxation of the monofilament fibers calculated at the third cycle of the dynamic testing with holding phase. The relaxation was calculated at high (35%) and low (15%) strains.

Filament	Mechanical Relaxation (%)		Electrical Relaxation (%)	
	High Strains	Low Strains	High Strains	Low Strains
Empa0.3	11.57	12.36	8.07	5.85
Empa0.5	23.05	28.64	12	7.51
Eel0.5	16.76	35.53	63.12	39.54

For the Empa0.5 the response was quite similar in comparison with the Empa0.3 monofilament. However, the values for relaxation both mechanical and electrical were higher.

Figure 8 presents the behavior of the Eel0.5 filaments during the quasi-static cycling test.

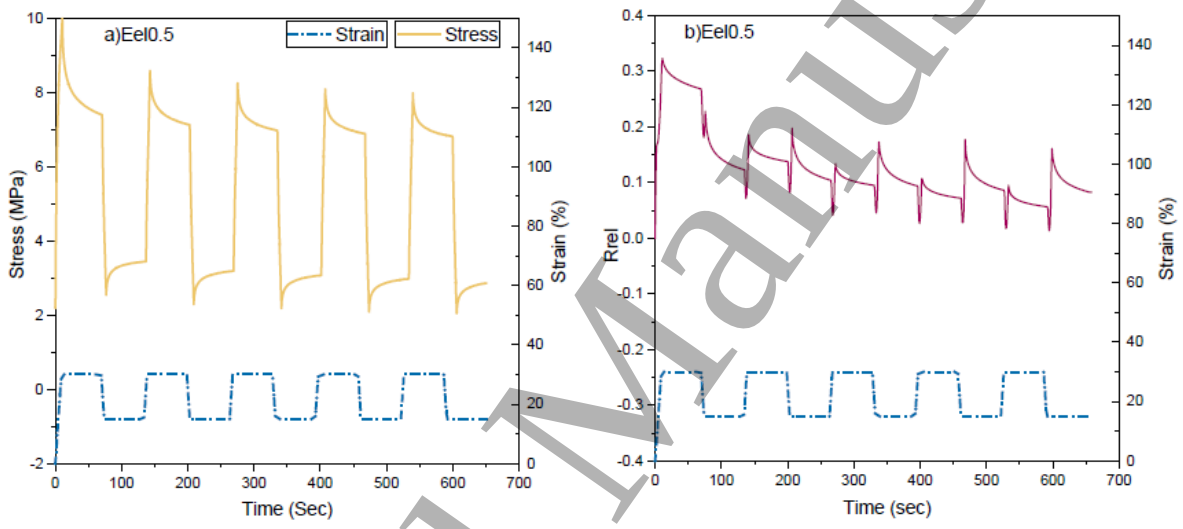

Figure 6: Quasi-static tensile testing, in a range of strains 15-35% with a holding phase of 60s between loading and releasing for the Empa monofilament filaments a) Stress Response for the Eel0.5 filament b) Relative resistance response for the Eel0.5

The stress signal shows a large relaxation and drift. In Figure 8b it can be observed, that the electrical signal also shows a significant relaxation and drift. Due to the high relaxation and drift, it is not possible to separate dwell time and unloading steps of the quasi-static measurement.

After the first cycle, it was not feasible to distinguish between the values of the relative resistance during the holding phase at low and at high strains. Comparing the results in table 1 and 2 it is obvious, that the Eel0.5 has much higher relative resistance relaxation and drift compared to the other two filaments.

4. Conclusion

In this study, commercially available and a self-developed piezoresistive thermoplastic elastomer materials for FDM (fused deposition modeling) printing processes have been investigated. To avoid effect on the piezoelectric properties of the conductive filaments, occurred by artifacts during FDM printing, single filaments were produced using a 3D printer and evaluated for their performance as strain sensors. The piezoresistive response of the different filaments was assessed by tensile testing with simultaneous measurement of the electrical resistance. For high strain rate, the Young's modulus

increased. High strain rate affected the sensor response and sensitivity of the filaments. That the Eel0.5 system had the lowest sensitivity even at the highest strain rate.

It was seen that between filaments with different diameter (Empa0.3 and Empa0.5), the piezoresistive response was different. For the filament Empa0.3 with the smaller diameter, better sensitivity and lower relaxation could be observed. The Eel0.5 showed the highest strain at the break but the electrical sensitivity is very low. During dynamic tensile testing, it was seen that the Eel filament was characterized by the appearance of a secondary plateau during the unloading and this loss of linear response will occur serious implications for applications were precise position monitoring is needed. The Empa filaments showed good sensitivity and dynamic response with low drift and good linearity during loading and unloading. Additionally, the Eel filament had significantly higher relaxation in the electrical signal compared to the Empa filaments during quasi-static cyclic testing.

Acknowledgment

This project has received funding from the European Union's Horizon 2020 research and innovation programme under grant agreement No 828818.

References

[1] Shih B, Christianson C, Gillespie K, Lee S, Mayeda J, Huo Z and Tolley M T 2019 Design Considerations for 3D Printed, Soft, Multimaterial Resistive Sensors for Soft Robotics *Front. Robot. AI* **6** 30

[2] White E L, Case J C and Kramer R K 2017 Multi-mode strain and curvature sensors for soft robotic applications *Sens. Actuators Phys.* **253** 188–97

[3] Rocha R P, Lopes P A, de Almeida A T, Tavakoli M and Majidi C 2018 Fabrication and characterization of bending and pressure sensors for a soft prosthetic hand *J. Micromechanics Microengineering* **28** 034001

[4] Mengüç Y, Park Y-L, Pei H, Vogt D, Aubin P M, Winchell E, Fluke L, Stirling L, Wood R J and Walsh C J 2014 Wearable soft sensing suit for human gait measurement *Int. J. Robot. Res.* **33** 1748–64

[5] Gong S, Lai D T H, Su B, Si K J, Ma Z, Yap L W, Guo P and Cheng W 2015 Highly Stretchy Black Gold E-Skin Nanopatches as Highly Sensitive Wearable Biomedical Sensors *Adv. Electron. Mater.* **1** 1400063

[6] Culha U, Nurzaman S G, Clemens F and Iida F 2014 SVAS(3): Strain Vector Aided Sensorization of Soft Structures *Sensors* **14** 12748–70

[7] Culha U, Wani U, Nurzaman S G, Clemens F and Iida F 2014 Motion Pattern Discrimination for Soft Robots with Morphologically Flexible Sensors *2014 IeeeRsj Int. Conf. Intell. Robots Syst. Iros 2014* 567–72

[8] Melnykowycz M, Tschudin M and Clemens F 2017 Piezoresistive Carbon-based Hybrid Sensor for Body-Mounted Biomedical Applications *4th Int. Conf. Compet. Mater. Technol. Process. Ic-Cmtp4* **175** UNSP 012006

[9] Turgut A, Tuhin M O, Toprakci O, Pasquinelli M A, Spontak R J and Toprakci H A K 2018 Thermoplastic Elastomer Systems Containing Carbon Nanofibers as Soft Piezoresistive Sensors *Acs Omega* **3** 12648–57

[10] Shen Z and Feng J 2019 Mass-produced SEBS/graphite nanoplatelet composites with a segregated structure for highly stretchable and recyclable strain sensors *J. Mater. Chem. C* **7** 9423–9

[11] Costa P, Goncalves S, Mora H, Carabineiro S a. C, Viana J C and Lanceros-Mendez S 2019 Highly Sensitive Piezoresistive Graphene-Based Stretchable Composites for Sensing Applications *Acs Appl. Mater. Interfaces* **11** 46286–95

[12] Liu H, Li Q, Zhang S, Yin R, Liu X, He Y, Dai K, Shan C, Guo J, Liu C, Shen C, Wang X, Wang N, Wang Z, Wei R and Guo Z 2018 Electrically conductive polymer composites for smart flexible strain sensors: a critical review *J. Mater. Chem. C* **6** 12121–41

[13] Rahim T N A T, Abdullah A M and Akil H M 2019 Recent Developments in Fused Deposition Modeling-Based 3D Printing of Polymers and Their Composites *Polym. Rev.* **59** 589–624

[14] Flandin L, Hiltner A and Baer E 2001 Interrelationships between electrical and mechanical properties of a carbon black-filled ethylene-octene elastomer *Polymer* **42** 827–38

[15] Segal E, Tchoudakov R, Narkis M and Siegmann A 2003 Sensing of liquids by electrically conductive immiscible polypropylene/thermoplastic polyurethane blends containing carbon black *J. Polym. Sci. Part B Polym. Phys.* **41** 1428–40

[16] Li G, Dai K, Ren M, Wang Y, Zheng G, Liu C and Shen C 2018 Aligned flexible conductive fibrous networks for highly sensitive, ultrastretchable and wearable strain sensors *J. Mater. Chem. C* **6** 6575–83

[17] Fan Q, Qin Z, Gao S, Wu Y, Pionteck J, Mäder E and Zhu M 2012 The use of a carbon nanotube layer on a polyurethane multifilament substrate for monitoring strains as large as 400% *Carbon* **50** 4085–92

[18] Tang Z, Jia S, Wang F, Bian C, Chen Y, Wang Y and Li B 2018 Highly Stretchable Core–Sheath Fibers via Wet-Spinning for Wearable Strain Sensors *ACS Appl. Mater. Interfaces* **10** 6624–35

[19] Mahfuz H, Adnan A, Rangari V K, Jeelani S and Jang B Z 2004 Carbon nanoparticles/whiskers reinforced composites and their tensile response *Compos. Part Appl. Sci. Manuf.* **35** 519–27

[20] Melnykowycz M, Tschudin M and Clemens F 2016 Piezoresistive Soft Condensed Matter Sensor for Body-Mounted Vital Function Applications *Sensors* **16**

[21] Mattmann C, Clemens F and Troester G 2008 Sensor for measuring strain in textile *Sensors* **8** 3719–32

[22] Clemens F J, Koll B, Graule T, Watras T, Binkowski M, Mattmann C and Silveira I Development of Piezoresistive Fiber Sensors, Based on Carbon Black Filled Thermoplastic Elastomer Compounds, for Textile Application *Advances in Science and Technology* **80** 7

[23] Costa P 2013 Electro-mechanical properties of triblock copolymer styrene–butadiene–styrene/carbon nanotube composites for large deformation sensor applications 10

[24] Wang X, Sun H, Yue X, Yu Y, Zheng G, Dai K, Liu C and Shen C 2018 A highly stretchable carbon nanotubes/thermoplastic polyurethane fiber-shaped strain sensor with porous structure for human motion monitoring *Compos. Sci. Technol.* **168** 126–32

[25] Liu H, Li Y, Dai K, Zheng G, Liu C, Shen C, Yan X, Guo J and Guo Z 2016 Electrically conductive thermoplastic elastomer nanocomposites at ultralow graphene loading levels for strain sensor applications *J. Mater. Chem. C* **4** 157–66

[26] Zheng Y, Li Y, Kun D, Mengran L, Zhou K, Guoqiang Z, Liu C and Shen C 2017 Conductive thermoplastic polyurethane composites with tunable piezoresistivity by modulating the filler dimensionality for flexible strain sensors 41–9

[27] Zhang R, Deng H, Valenca R, Jin J, Fu Q, Bilotti E and Peijs T 2013 Strain sensing behaviour of elastomeric composite films containing carbon nanotubes under cyclic loading *Compos. Sci. Technol.* 5

[28] Ji M, Deng H, Yan D, Li X, Duan L and Fu Q 2014 Selective localization of multi-walled carbon nanotubes in thermoplastic elastomer blends: An effective method for tunable resistivity–strain sensing behavior *Compos. Sci. Technol.* **92** 16–26

[29] Drozdov A D and Christiansen J 2009 Thermo-viscoplasticity of carbon black-reinforced thermoplastic elastomers *Int. J. Solids Struct.* 11

[30] Yamada T, Hayamizu Y, Yamamoto Y, Yomogida Y, Izadi-Najafabadi A, Futaba D N and Hata K 2011 A stretchable carbon nanotube strain sensor for human-motion detection *Nat. Nanotechnol.* **6** 296–301

[31] Duty C, Ajinjeru C, Kishore V, Compton B, Hmeidat N, Chen X, Liu P, Hassen A A, Lindahl J and Kunc V 2018 What makes a material printable? A viscoelastic model for extrusion-based 3D printing of polymers *J. Manuf. Process.* **35** 526–37

[32] Talataisong W, Ismaeel R, Sandoghchi S R, Rutirawut T, Topley G, Beresna M and Brambilla G 2018 Novel method for manufacturing optical fiber: extrusion and drawing of microstructured polymer optical fibers from a 3D printer *Opt. Express* **26** 32007

[33] Ninjatek Eel 3D Filament Safety Data Sheet, 2018, Fenner Drives

[34] Hussein M 2018 Effects of strain rate and temperature on the mechanical behavior of carbon black reinforced elastomers based on butyl rubber and high molecular weight polyethylene | Elsevier Enhanced Reader *Results in Physics* **9**

[35] Qi H J and Boyce M C 2005 Stress–strain behavior of thermoplastic polyurethanes *Mech. Mater.* **37** 817–39

[36] Flandin L, Bréchet Y and Cavaillé J-Y 2001 Electrically conductive polymer nanocomposites as deformation sensors *Compos. Sci. Technol.* **61** 895–901

[37] Duan L, Fu S, Deng H, Zhang Q, Wang K, Chen F and Fu Q 2014 The resistivity-strain behavior of conductive polymer composites: stability and sensitivity *J. Mater. Chem. A* **2** 17085–98

[38] Tang Z, Jia S, Shi X, Li B and Zhou C 2019 Coaxial Printing of Silicone Elastomer Composite Fibers for Stretchable and Wearable Piezoresistive Sensors *Polymers* **11** 666

[39] Wang L, Ding T and Wang P 2009 Research on stress and electrical resistance of skin-sensing silicone rubber/carbon black nanocomposite during decompressive stress relaxation *Smart Mater. Struct.* **18** 065002